Mon. Not. R. Astron. Soc. **000**, 000–000 (0000) Printed 5 August 1999 (MN LaTeX style file v1.4)

Detection of the optical counterpart of the proposed double degenerate polar RX J1914+24

Gavin Ramsay[1], Mark Cropper[1], Kinwah Wu[2], K. O. Mason[1], Pasi Hakala[3]
[1] *Mullard Space Science Laboratory, University College London, Holmbury St. Mary, Dorking, Surrey RH5 6NT*
[2] *Research Centre for Theoretical Astrophysics, School of Physics, University of Sydney, NSW 2006, Australia*
[3] *Observatory and Astrophysics Lab, FIN-00014, Univ Helsinki, Helsinki, Finland*

Received:

ABSTRACT

We have detected the optical counterpart of the proposed double degenerate polar RX J1914+24. The I band light curve is modulated on the 9.5 min period seen in X-rays. There is no evidence for any other periods. No significant modulation is seen in J. The infrared colours of RX J1914+24 are not consistent with a main sequence dwarf secondary star. Our *ASCA* spectrum of RX J1914+24 is typical of a heavily absorbed polar and our *ASCA* light curve also shows only the 9.5 min period. We find that the folded I band and X-ray light curves are out of phase. We attribute the I band flux to the irradiated face of the donor star. The long term X-ray light curve shows a variation in the observed flux of up to an order of magnitude. These observations strengthen the view that RX J1914+24 is indeed the first double degenerate polar to be detected. In this light, we discuss the synchronising mechanisms in such a close binary and other system parameters.

Key words: Accretion, Cataclysmic variables, X-rays: stars, Stars: individual: RX J1914+24.

1 INTRODUCTION

Cropper et al. (1998) reported X-ray observations of the cataclysmic variable (CV) RX J1914+24 which was discovered by Motch et al. (1996) in the *ROSAT* All-Sky Survey. Motch et al also found that the X-ray flux was modulated at 9.5 min (= 569 sec). This period is characteristic of Intermediate polars (IPs: the non-synchronous magnetic CVs, Patterson 1994), but the shape of the folded light curve showed no X-ray flux for approximately half the 9.5 min period. This property is difficult to reconcile with our current understanding of IPs. Given the absence of any other periods, Cropper et al. (1998) suggested that RX J1914+24 was a polar, or AM Her system – the synchronous magnetic CVs (Cropper 1990, Beuermann & Burwitz 1995). This would imply that the binary orbital period is 9.5 min.

An orbital period of 9.5 min would be the shortest period of any known binary star. It would also exclude the secondary from being a main-sequence star (the shortest period allowed is $\sim$ 80 min). For a non-degenerate He burning secondary, the minimum orbital period is $\sim$ 13 min (Iben & Tutukov 1991). However, a degenerate He secondary can have a period in the range $\sim$ 6 – 50 min (Tutukov & Yungelson 1996). Confirmation that RX J1914+24 is a double-degenerate polar would have important implications for how magnetic binaries evolve. It would also be the first known magnetic system in which the accretion flow was predominately He dominated.

Comparison between the X-ray position of RX J1914+24 (determined using the High Resolution Imager, HRI, on *ROSAT*) and the optical image of Motch et al (1996) showed that star 'H' was the most likely optical counterpart (Cropper et al 1998). This star is heavily reddened ($A_V \sim 5.6$: Motch et al 1996). To detect the optical counterpart of RX J1914+24 and search for periods other than the 9.5 min period seen in X-rays we have obtained images of the field of RX J1914+24 in the I band and at IR wavelengths, the rationale being that if no other periods were seen then this would strengthen the conclusion of Cropper et al. (1998) that RX J1914+24 is a double degenerate polar. We also report another set of X-ray data obtained using *ROSAT* and one obtained using *ASCA*.

2 X-RAY OBSERVATIONS

2.1 *ROSAT* Data

Cropper et al (1998) presented X-ray observations of RX J1914+24 taken using *ROSAT* (0.1–2.0keV) at 3 distinct epochs. While the shape of the folded light curve was similar at each epoch, the peak intensity varies over time. To monitor the shape and intensity of the X-ray light curve we obtained a further set of data using the *ROSAT* HRI in Oct 1997 with a the total exposure of 21.5ksec. We extracted a background subtracted light curve in the same way as Cropper et al. (1998) and show it along with the other *ROSAT* data in Fig.1. We also show the folded light curve of the HRI data taken in Oct 1995 which was not shown in Cropper et al. (1998) as the exposure time was only 2.4ksec. These data show a range of maximum brightness: using a spectrum similar to that found in §2.2 for the *ASCA* data, the system was a factor of ∼3 fainter in Sept 1993 compared to that in Apr 1996.

The data shown in Fig.1 were folded on the linear ephemeris obtained by fitting the start of the rise from zero flux. From 4 epochs we obtained 108 timings. This gave a best fit ephemeris:

$$T_o = \mathrm{HJD}\ 2449258.03941(6) + 0.0065902334(4)$$

The numbers in brackets give the standard error on the last digit. This allows us to phase all our data from Sept 1993 to July 1998 within 0.02 cycles.

2.2 *ASCA* observations

We obtained a 20ksec observation of RX J1914+24 in 1998 April 9–10 using *ASCA* (∼0.5–10keV). The data were extracted by applying the standard data selection criteria. The background was generated using a concentric annulus around the source. RX J1914+24 was detected only in the SIS detector and only below 1keV. The light curve from the SIS0 detectors (the peak flux of the folded SIS1 data is approximately half that of SIS0) were analysed using a Discrete Fourier Transform code (DFT; Deeming 1975, Kurtz 1985). The amplitude spectrum is shown in Fig. 2: the most prominent amplitude peak corresponds to the 9.5 min period seen in the *ROSAT* data. The amplitude spectrum prewhitened by the 9.5 min period (and harmonic) is also shown in Fig.2. There is no evidence for a significant modulation at any other period.

The light curve derived from the SIS0 data was folded on the ephemeris determined in §2.1. We show the folded light curve in Fig. 1. The shape of the light curve during the bright phase is more peaked than the *ROSAT* HRI data taken in Oct 1997 but similar to that taken in Apr 1996. Using the spectral parameters found below we find that RX J1914+24 was fainter in X-rays by a factor of ∼3 at the epoch of the *ASCA* observation compared with Oct 1997.

The *ASCA* spectrum (Fig. 3) could be fitted reasonably well (the best fit gave $\chi^2 = 1.31$, 20 degrees of freedom), with a low temperature (kT ∼40eV) blackbody plus interstellar absorption ($N_H \sim 1 \times 10^{22}$ cm^{-2}). The temperature and absorption were not well constrained. The upper limit (90 percent confidence) to a thermal bremsstrahlung component (using an assumed temperature of 10keV) corresponds to a 2–10 keV flux of 7.8×10^{-14} erg cm^{-2} s^{-1} (9×10^{28} erg s^{-1} at 100pc). The bolometric luminosity of the blackbody component is $\sim 1 \times 10^{36}$ erg s^{-1} at 100pc. This agrees very well with the estimate derived from the *ROSAT* spectrum (Cropper et al 1998). The low flux from the bremsstrahlung component and the very large ratio between the soft blackbody component and the hard bremsstrahlung component is typical of polars (eg Ramsay et al 1994). X-ray spectra of

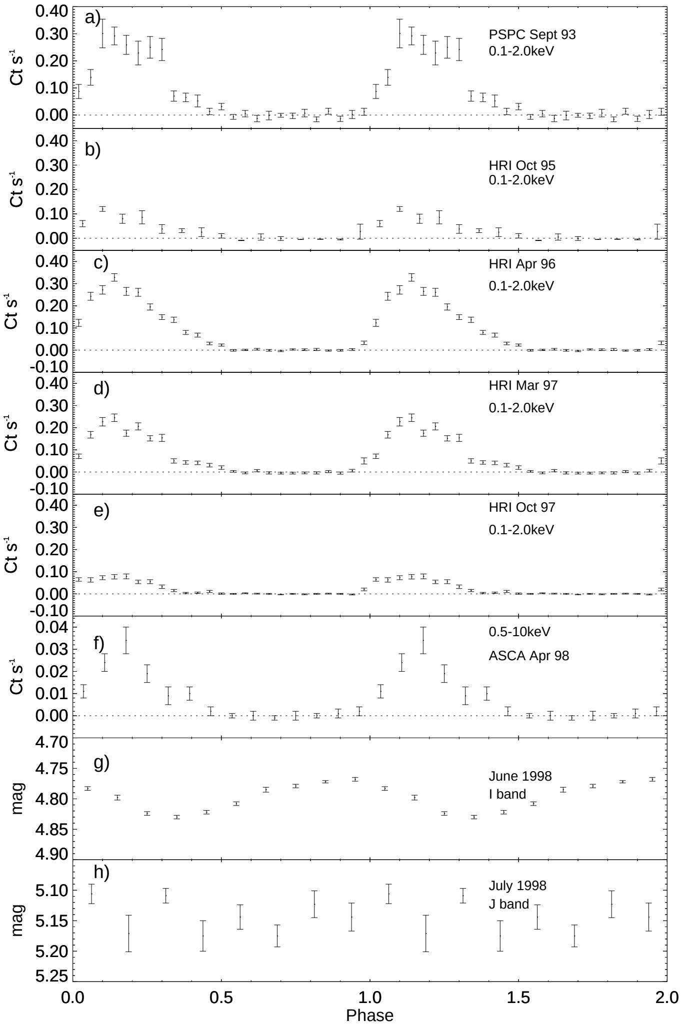

Figure 1. Panels a)–e): the *ROSAT* data from different epochs, Panel f): the ASCA data, Panel g) the I band data obtained using NOT and Panel h): J band data obtained using UKIRT.

IPs typically have a strong medium energy component and rarely show a strong soft component.

3 OPTICAL-IR OBSERVATIONS

3.1 *I* band polarimetry

Observations were obtained on the nights 1998 June 25 – 27 using the 2.5-m Nordic Optical Telescope (NOT) on La Palma and the Andalucia Faint Object Spectrograph and Camera (ALFOSC) used in its imaging mode. On the first night, data were obtained over 7hrs 26min while this figure was 4hrs 19min and 7hrs 55mins on the second and third nights respectively. The conditions were good and the seeing was typically 1$''$ or better. To obtain circular polarimetry data a 1/4 waveplate was inserted into the optical path: this split the light into o and e rays on the Loral 2k×2k CCD so that 2 images of each star were recorded. The instrument was orientated in such a way that images of field stars did

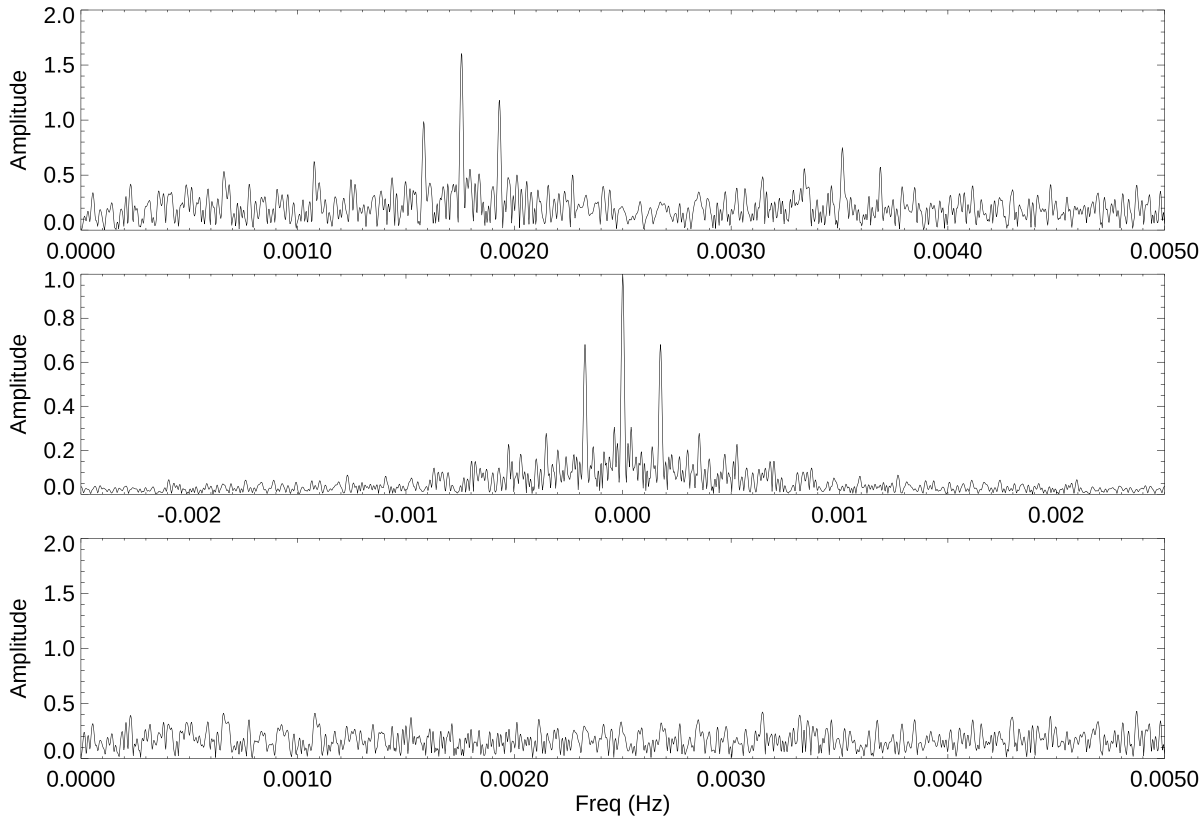

Figure 2. The amplitude spectrum (top) of the *ASCA* SIS0 data, the window function (middle) and the amplitude spectrum pre-whitened by the 569 sec period (lower).

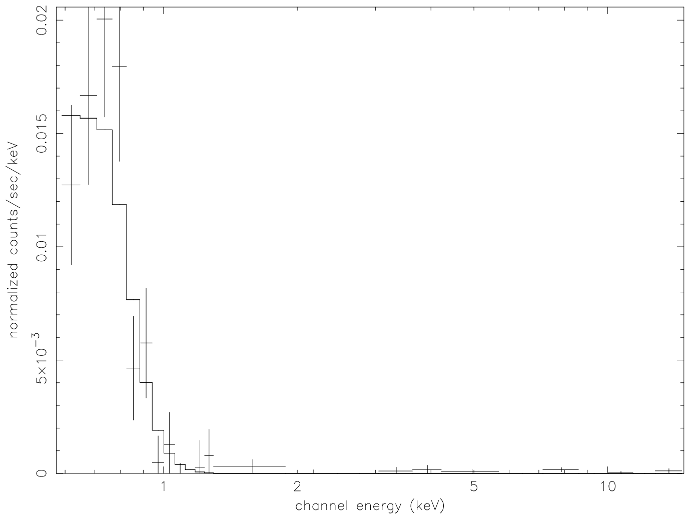

Figure 3. The integrated *ASCA* SIS-0 spectrum together with the best fitting absorbed blackbody model.

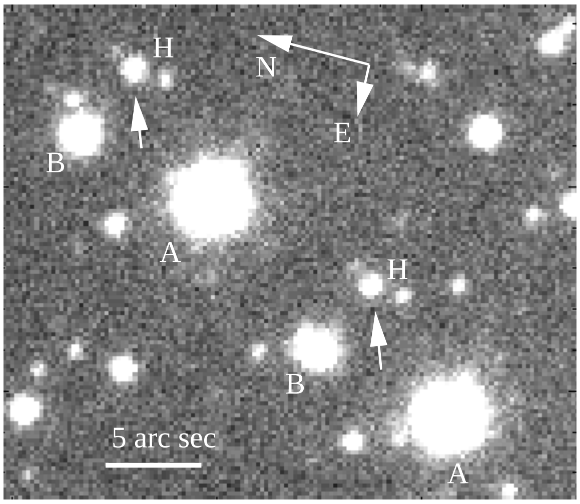

Figure 4. An I band image of the field of RX J1914+24 taken in June 1998 using NOT. Two images of the each object in the field are recorded – one from each polarised ray. Stars 'A' and 'B' in the finding chart of Motch et al. (1996) are shown. RX J1914+24 is marked by an arrow. Star 'H' of Motch et al. is thus a blend of more than 1 star (including RX J1914+24).

not overlap with any of the stars of interest. The images were bias subtracted and flat fielded. A typical image is shown in Fig.4. In the I band finding chart of Motch et al. (1996) star 'H' is shown as a single star: in our I band images (which were taken under good seeing) we find that star 'H' is made up of more than one star. This is consistent with our K band image taken using UKIRT in service time in October 1997.

Profile fitting photometry was carried out on the stars in the field using `DAOPHOT` (Stetson 1992). Since the profiles of the stellar images in the o and e rays differed, two profiles had to be constructed – one for each ray. We obtained differential photometry between Star 'A' and the stars in the immediate vicinity of star 'H' and Fourier Transformed their light curves. The brightest component making up star 'H' was found to show a significant amplitude peak at 9.5 min in both the 'upper' and 'lower' polarised beams (see Fig. 5). This period corresponds to the period found in X-rays: this star is therefore the optical counterpart of RX J1914+24 (arrowed in Fig.4). Neither star 'B' nor the fainter component of star 'H' were found to show any significant modulation. Whilst there are minor amplitude peaks at longer periods in both the 'upper' and 'lower' amplitude spectra, there is no peak which is seen in both spectra: therefore we conclude that these peaks are not significant.

We folded the I band optical data of RX J1914+24 on the ephemeris in §2.1. These data are also shown in Fig.1. The peak-to-peak amplitude is $\sim$ 0.07 mag and the mean magnitude is $I \sim 18.2$ assuming the magnitude of star 'A' is $I \sim 13.4$ (Motch et al. 1996). This contrasts with the approximate magnitude of star 'H' as seen by Motch et al. in June 1993 of 16.6 mag. Even taking into account that star 'H' is consists of more than 1 component, (RX J1914+24 being 18.2 mag, the next brightest $\sim$ 19.6), RX J1914+24 was over 1 mag fainter in I in June 1998 compared to June 1993.

If there is a second period hidden the I band data then its amplitude must be very small. From the noise level in the amplitude spectrum (Fig. 5), any second period shorter than $\sim$5 hrs must have a peak-to-peak amplitude less than 0.02 mag. This is much less than the variation generally seen in I band photometry of other magnetic CVs. For example in the case of the IP YY Dra, the orbital period of 3.97 hrs is clearly seen as a modulation with an amplitude of 0.12 mag in the I band (Haswell et al 1997). Since YY Dra is expected to have an accretion disc, the modulation of the secondary star will be diluted by the presence of a disc. In the case of discless systems such as RX J1914+24 (cf §8.1), the amplitude is expected to be greater. For instance I band photometry of the polar V895 Cen in a low state (where there is no additional flux from cyclotron emission) shows a peak to peak amplitude of $\sim$0.4 (Stobie et al 1996). The lack of such a pronounced modulation in RX J1914+24 is further evidence that the secondary star in this system is not a main sequence star.

The 1/4 waveplate and calcite block in the optical path allowed us to search for circular polarisation in RX J1914+24. The circular polarisation was derived for stars 'A' and 'B' in the finding chart of Motch et al. (1996) and also RX J1914+24. The instrumental polarisation was found to depend on the position of the stellar image on the CCD. We made a first order correction for instrumental polarisation based on the assumption that star 'A' has no intrinsic circular polarisation. The corrected data of star 'B' and RX J1914+24 were then folded on the ephemeris derived in §2.1 and are shown in Fig. 6. Star 'B' shows a small net negative circular polarisation indicating that there is probably some small residual effects of the polarisation varying on the field position. In the case of RX J1914+24 there is a small positive ($\sim$ 0.3 per cent) residual polarisation, although there is no significant modulation over the 9.5 min period. We conclude that there is no intrinsic circularly polarised emission from RX J1914+24 in the I band.

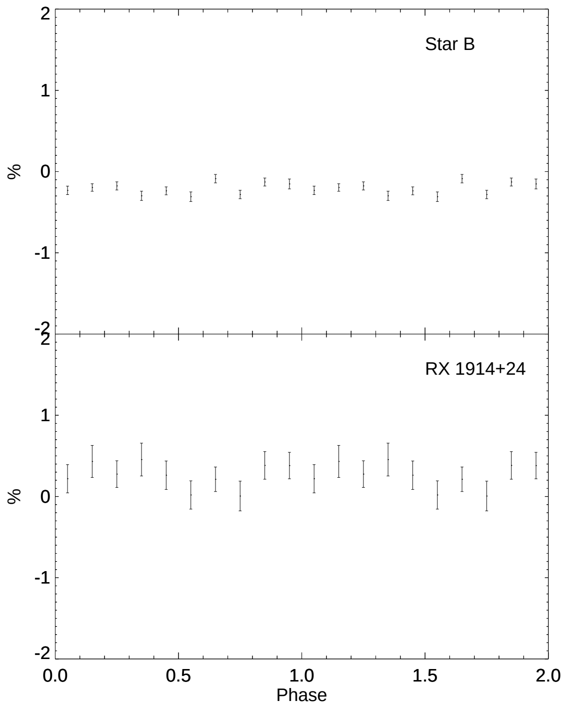

Figure 6. The circular polarisation data for star 'B' in the finding chart of Motch et al. (1996) and RX J1914+24. The unfolded data were corrected by setting the circular polarisation for star 'A' to zero. The corrected data were then folded on the ephemeris derived in §2.1.

3.2 Infrared Photometry

RX J1914+24 was observed using UKIRT on Mauna Kea on the nights 1998 July 2 – 3 mainly in the J band, but images were also obtained in H and K. On the first night conditions were good but in the second half of the second night conditions were poor and unusable. Images were obtained using IRCAM3 operating in ND_STARE mode. In the J band, a 12 sec exposure was made then the telescope was shifted: this allowed us to make a flat field. Each resulting image was the result of 6 exposures.

Profile fitting was performed on the stars in each image using `DAOPHOT` (Stetson 1992). As with the NOT data, differential photometry was performed on star 'B' and the optical counterpart of RX J1914+24 using star 'A' as the comparison. The differential light curves were Fourier Transformed. The amplitude spectrum of RX J1914+24 is shown in Fig.7: no significant modulations were seen in the light curves of either RX J1914+24 or star 'B'. In the case of RX J1914+24 we folded the differential photometry on the ephemeris shown in §2.1 as shown in Fig.1. As expected from the amplitude spectrum there is no evidence for a significant modulation on the 9.5 min period. However, the scatter is much greater than the folded I band light curve and it is possible that a modulation similar to that seen in I is hidden in the noise.

What amplitude to we expect to see in the J band in normal CVs with a main sequence secondary stars? A modulation of $\sim$0.4 mag is seen in the IP FO Aqr (de Martino et al 1994), while no significant modulation (<0.08 mag) is seen in the IP RX J1238-38 (Buckley et al 1998) which at

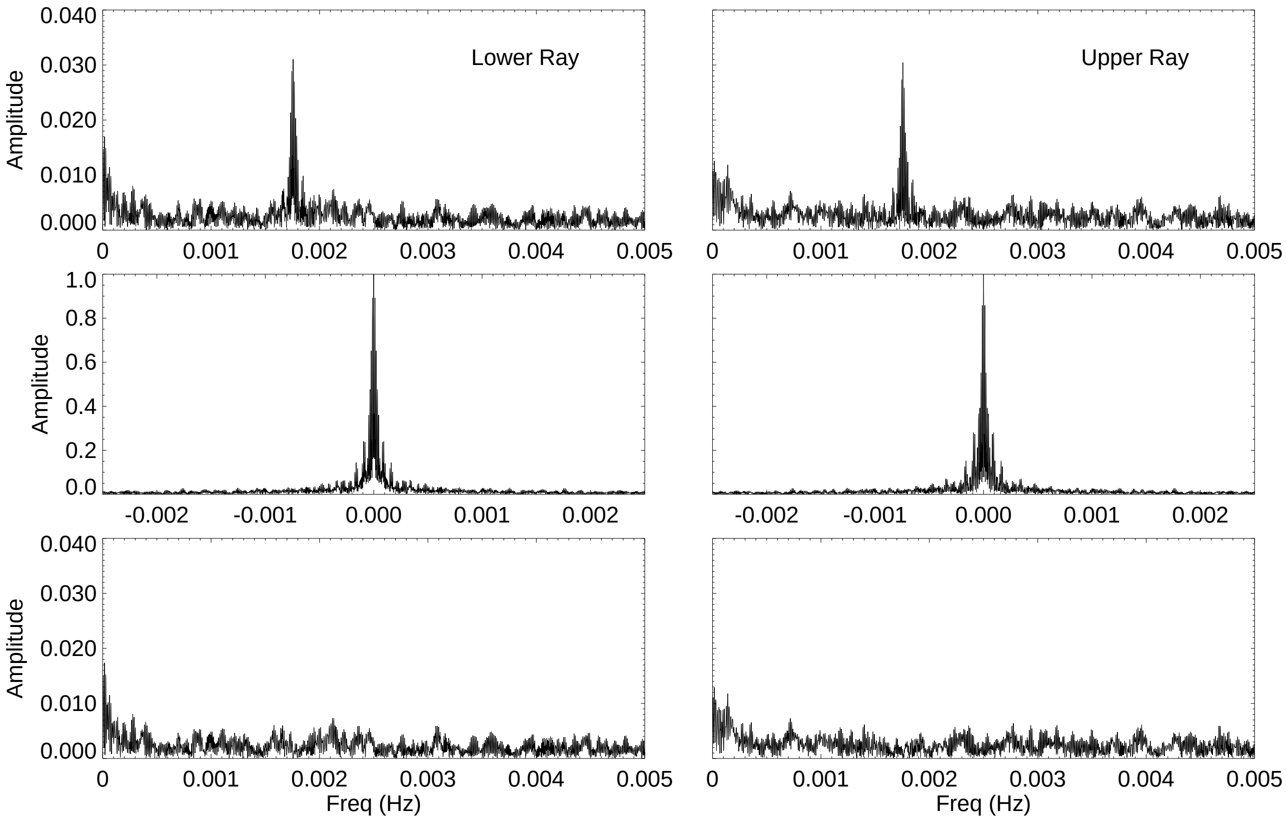

Figure 5. The amplitude spectra from the lower and upper polarised images of the brightest component of star 'H' are shown in the top panel. The prominent amplitude peak corresponds to the 569-sec (9.5-min) period seen in X-rays. The middle panel shows their window functions and the lower panel shows their amplitude spectra pre-whitened by the 569-sec period.

an orbital period of 84 min is below the period gap. From the noise level of the amplitude spectrum of the J band photometry (Fig. 7), the upper limit for a modulation is an order of magnitude lower than observed in RX J1238-38. We conclude that this is a very low level for a main sequence secondary star.

In addition to the J band data we also obtained single images in H and K bands. As before, differential photometry was performed between the optical counterpart of RX J1914+24 and star 'A' and 'B'. These differential magnitudes were placed onto the standard systems from observations of faint UKIRT standard stars. Table 1 shows the reduced magnitudes. We also show the dereddend magnitudes and fluxes assuming an extinction of A_V=5.6 mag (Cropper et al 1998). This corresponds to A_I=2.72, A_J=1.59, A_H=0.97 and A_K=0.63 assuming R=3.1 and the observed ratios in Fitzpatrick (1999). The K observed magnitude of 17.1 compares with 16.4 when we obtained our service observation in Oct 1997.

Band	Mean Magnitude	Dereddened Magnitude	Dereddened Flux erg cm^{-2} s^{-1} Å^{-1}
I	18.2±0.05	15.5	$8.1\pm0.3 \times 10^{-16}$
J	17.3±0.10	15.7	$1.7\pm0.2 \times 10^{-16}$
H	17.4±0.15	16.4	$3.3\pm0.06 \times 10^{-17}$
K	17.1±0.15	16.5	$1.0\pm0.06 \times 10^{-17}$

Table 1. The apparent, together with the dereddened magnitudes and dereddened fluxes of RX J1914+24 assuming an extinction of A_V = 5.6 mag on 1998 July 2,3. The error on the mean magnitudes includes the error in placing them onto the standard system. The error on the dereddened flux does not include the uncertainty on the extinction.

4 THE OPTICAL NEAR-IR FLUX

The dereddend colours in Table 1 do not depend greatly on the precise value of the assumed extinction. Decreasing the extinction from A_V=5.6 to 5.0 changes the colours $(I-K)$, $(J-H)$ and $(H-K)$ by 0.17, 0.06 and 0.03 mag respectively. To compare the dereddend infrared colours of RX J1914+24 with late-type dwarf stars we show in Fig.8 the colours of RX J1914+24 in the $(I-K)$, $(J-H)$ and $(I-K)$, $(H-K)$ planes together with old disk dwarfs with spectral types K7 to M7.5 (Bessell 1991). It is clear that the dereddened infrared colours of RX J1914+24 are not consistent with a dwarf late main sequence secondary star. (We should add a note of caution at this stage that our I band observations were not simultaneous with our JHK observations, but were earlier by a week).

We now use the dereddend fluxes shown in Table 1 to estimate whether the spectral continuum could be fitted with a simple blackbody model as would be roughly the case for a low temperature white dwarf. The errors in our data increase rapidly from K towards I, since they are dominated by the uncertainty in the amount of reddening involved (the errors shown in Fig. 9 include the uncertainty in the photometric mean magnitude and also an uncertainty in the extinction

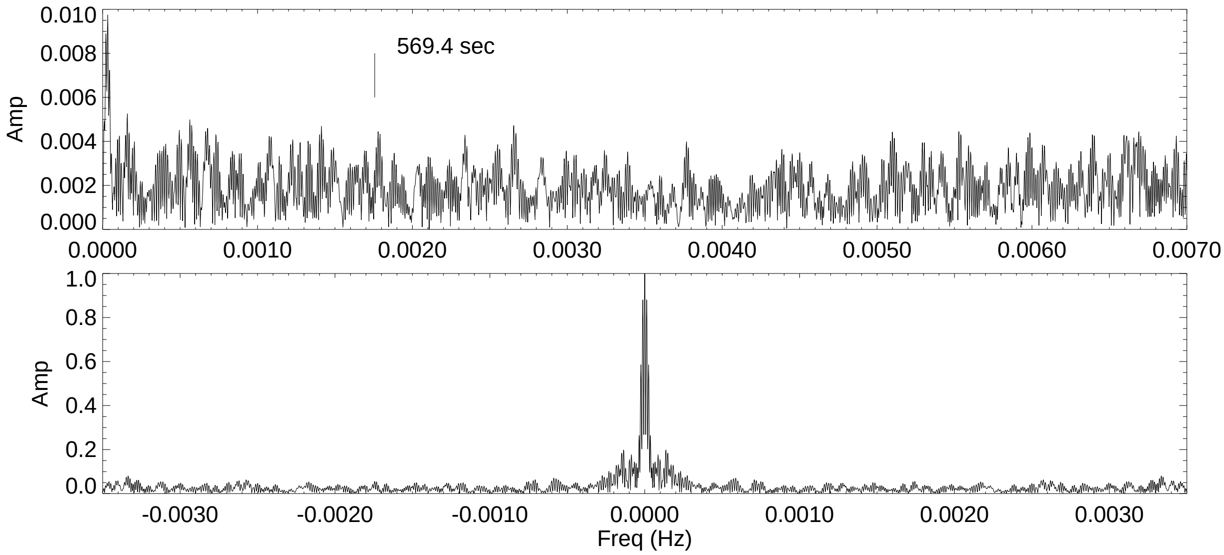

Figure 7. The amplitude and window spectrum for the J band light curve obtained at UKIRT. The 569.4 sec marker shows the period of RX J1914+24 found in X-rays.

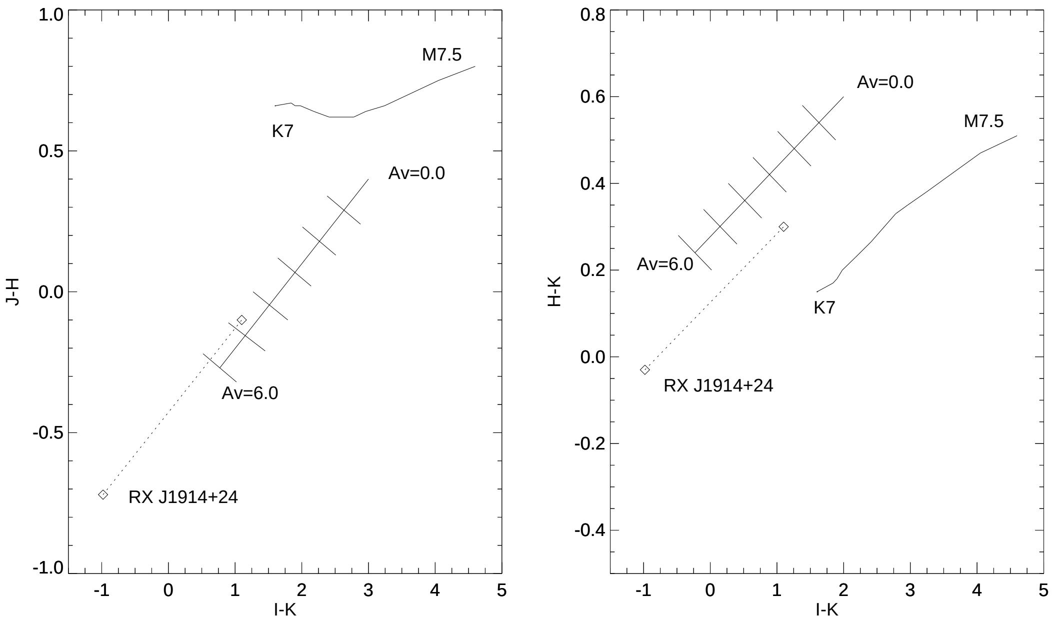

Figure 8. The position of RX J1914+24 in the observed and dereddened colours in the $(I-K)$, $(J-H)$ and $(I-K)$, $(H-K)$ planes. The positions of old disk M dwarfs with spectral types K7 to M7.5 are also shown (Bessell 1991). The ticked line shows the reddening direction for A_V=0.0 to 6.0 in steps of 1.0.

of A_V =0.5). Despite this, it is clear from our blackbody fits, plotted in Fig. 9, that the spectrum is far too hot to be explained simply by the blackbody component alone. In Fig. 9 we show the data and three fixed temperature blackbody fits. No satisfactory blackbody fit was found to fit the data well, although a higher temperature fit is less poor than a cooler one. If the blackbody temperature is left as a free parameter in the fit, it will tend towards infinity. Were we to assume that the extinction towards RX J1914+24 was lower than A_V =5.6, (say A_V =4.0) then we can obtain a good fit and lower temperature (~13000K).

Taking the extinction found by fitting the X-ray spectra as representative of the optical extinction, these results suggest that in the optical-IR region of the spectrum there is a component additional to a blackbody, which adds to the emission at shorter wavelengths. This could be due to emission from the accretion stream, cyclotron emission from the

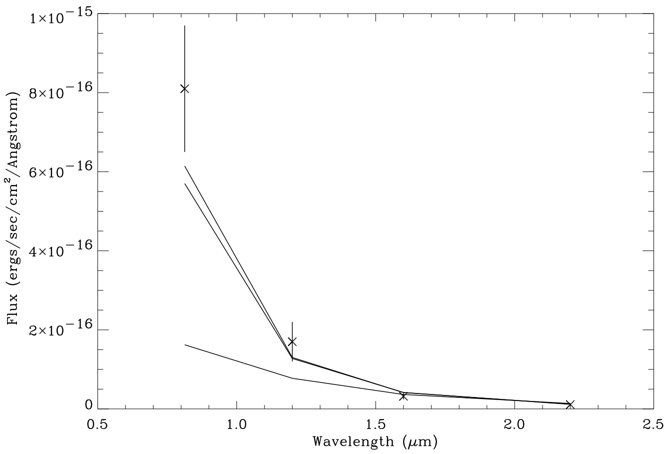

Figure 9. The dereddened fluxes and three fixed temperature blackbody fits. These correspond to blackbody temperatures (from top to bottom) of 500000K, 50000K and 5000K respectively.

white dwarf or an irradiated component on the donor white dwarf. We now address these possibilities in turn.

Although we cannot exclude emission from a hot accretion stream this seems unlikely because the I band folded light curve (Fig. 1) would be double peaked unless we are viewing the system at a low inclination. For a magnetic field of a few MG (see below) the optically thin (and hence polarised) part of the cyclotron spectrum is likely to be in red wavebands. Since we do not observe a significant circularly polarised flux in I the magnetic field is either stronger than we expect (in which case the optically thin cyclotron harmonics would be in the UV) or it is very low (in which case the optically thin cyclotron harmonics would be in the far IR). On the other hand it is also possible that a shock does not form above the accretion region on the primary white dwarf because of the small dimensions of the system.

Because the binary components are unusually close, we expect the secondary white dwarf to intercept an appreciable part of the accretion flux. Observations of conventional polars show that the irradiated surface of the secondary is brighter in the trailing hemisphere (eg Southwell et al 1995). Assuming that the irradiated surface is much larger than the accretion region on the primary star, then this would imply that the I band flux peaks between $\phi \sim$0.2–0.6 cycles after the X-ray peak – which is indeed what we observe (Fig. 1). We conclude therefore that the variation in I is probably due to irradiation of the secondary by the X-rays produced at the accretion region on the primary star.

If this is indeed the case, then we can also make the assumption that the origin of the 9.5 min period seen in the I band amplitude spectrum (Fig. 5) is caused by the secondary star. On the other hand the 9.5 min period seen in the *ASCA* amplitude spectrum (Fig. 2) is due to the accretion region on the white dwarf. The fact that the amplitude peaks in the *ASCA* and I band amplitude spectra are indistinguishable is further evidence that RX J1914+24 is synchronised.

5 THE MASS OF THE SECONDARY STAR

For semi-detached binaries, the Roche-lobe-filling condition implies a unique relation between the average density of the donor star and the binary orbital period (see eg Frank, King & Raine 1992, eqn 4.8). Assuming that the 9.5-min period detected in RX J1914+24 is indeed the orbital period and that the Roche lobe approximation is valid for degenerate stars, the average density of the secondary star will be about 4600 g cm^{-3}. The typical density of a main-sequence star is $\sim$ 100 g cm^{-3}. Thus, the deduced high density of the secondary star immediately places it into the class of degenerate dwarfs. Using the Nauenberg (1972) mass-radius relation for white dwarfs and the Eggleton (1983) approximation for the Roche-lobe volume radius, we estimate that the mass of the secondary star is about 0.08 $M_\odot$.

6 THE DISTANCE TO RX J1914+24

If we assume for the sake of argument the 9.5-min seen in RX J1914+24 is the spin period and there is a second period (the orbital period) which has been missed for some reason (ie the system is an IP) – what would the minimum distance be to the system? Taking the empirical relation for the spin and the orbital periods for IPs

$$P_{\rm orb} \approx 10 P_{\rm spin} \quad (1)$$

(Barrett, O'Donoghue & Warner 1988), we estimate that the orbital period would be $\approx$ 95 min. If the secondary star is a main-sequence star filling its Roche lobe, a 95-min orbital period implies a mass and radius of 0.12 $M_\odot$ and 0.16 $R_\odot$ respectively (eg Warner 1995).

Bailey (1981) derived a surface brightness relationship

$$S_K = K + 5 - 5\ \log D + 5\ \log r_2\ , \quad (2)$$

from which we can deduce the distance if the surface brightness of the star in the K band (S_K), the distance (D, in pc) and the radius of the secondary star (r_2, in solar units) are known. The mass and radius of the secondary star in RX J1914+24, deduced from the assumed 95-min orbital period, implies a spectral type of K7 – M3 for the star. We have already noted that this is not consistent with our IR colours. For main sequence stars, $S_K \sim 4.4$ (Ramseyer 1994). Using the de-reddend K magnitude in table 1, we obtain a value of 310 pc for the lower limit to distance of RX J1914+24. This distance is consistent with the mean distance of known CVs. However, if RX J1914+24 is at a distance of 310 pc, the bolometric luminosity given in Cropper et al. (1998) should be increased by a factor of ∼10. Then the mass transfer rate of the system is now as high as 6×10^{-6} $M_\odot$/yr. Such a high mass transfer rate is difficult to be explained by current orbital evolution theories. We therefore consider this as further evidence for a double degenerate interpretation. If we have a longer orbital period, ie $P_{\rm orb} > 10 P_{\rm spin}$, then this problem is significantly worse.

We now go on to determine a distance based on the measurement of the extinction to RX J1914+24. The solar system lies in a region of space which has a lower hydrogen density compared to the surrounding region (eg Warwick et al 1993). The distance to the edge of this low density region depends on the direction. This has been determined, for instance, by the distribution in the sky of white dwarfs visible in the soft X-ray band (eg Barstow et al 1997). Because the X-ray spectrum of RX J1914+24 is heavily reddend (§2.2), this implies that it is at a distance greater than the distance to the edge of the low density region. Using the map of distance to the edge of the low density region as a function of galactic co-ordinates in Barstow et al (1997) we find that the distance to RX J1914+24 is greater than ~100pc, assuming that the absorption we observe is not internal to the binary system.

If we assume that the I band flux can be characterised by a blackbody, we find that a blackbody with the volume of a secondary Roche lobe for a 9.5 min period will give the dereddend I band flux (Table 1) at a distance of 100pc if it has a temperature of ~9500K. For a distance of 400pc we need to increase the temperature to ~60000K to match the dereddend I band flux. While caution should be exercised when comparing the temperatures of accreting white dwarfs with non accreting white dwarfs (since the latter have no external heat source), non accreting white dwarfs generally have temperatures $\lesssim$60000K (Barstow et al 1993). Whilst there is some uncertainty regarding the appropriateness of adopting a blackbody, it nevertheless suggests that RX J1914+24 lies at a distance of ~100–400pc. If there is significant heating of the secondary in the form of irradiation, then the upper limit will be less than 400pc.

7 LONG TERM VARIATIONS IN INTENSITY

In Fig. 1 we show the X-ray folded light curves taken at various epochs over a space of 5 years. To compare the peak count rate using *ROSAT* PSPC and *ASCA* to that of the *ROSAT* HRI we used the best fit spectral parameters of fitting the *ASCA* spectrum with an absorbed blackbody (§2.2). The equivalent HRI count rate as a function of time is shown in Fig. 10. We find that the X-ray flux varies by approximately an order of magnitude. If this X-ray variation is reflected in the optical-IR flux then this would correspond to a range in optical brightness of 2.5 magnitudes. This is similar to the range seen in the long term optical light curve of the polar AM Her (Feigelson, Dexter & Liller 1978). On the other hand, IPs (which have a reservoir of material in the form of a disk), do not (in general) show such a large range in brightness. We also show the I and K band magnitudes at two epochs which are broadly consistent with the change in the X-ray flux. There is no evidence for a correlation between the shape of the light curve (Fig. 1) and the intensity.

The most obvious cause for the long term intensity changes is a variation in the mass transfer rate. In conventional polars various schemes have been proposed to explain these variations although none have been fully developed. One such scheme is that of magnetic activity, such as star spots, near the L_1 point on the secondary somehow affects $\dot{M}$(eg Barrett, O'Donoghue & Warner 1988, Livio & Pringle 1994).

8 DISCUSSION

Cropper et al. (1998) argued that RX J1914+24 was a double degenerate polar to account for the lack of a second period in the *ROSAT* data and the shape of the X-ray light curve. This is supported by our I band and *ASCA* light curves and by the lack of any variation at any other period in the J band. Further the long term X-ray light curve and the *ASCA* spectrum is typical of polars. These observations reinforce the proposal of Cropper et al. (1998) that RX J1914+24 is a double degenerate polar. We now go on to discuss system parameters such as the primary stars magnetic field strength and the forces which would be needed to keep RX J1914+24 synchronised.

8.1 Lower limit to the primary's magnetic field

As no other periods apart from the 9.5 min period have been detected in either the X-ray or I band light curves, we conclude that RX J1914+24 does not have an accretion disk. For accreting white dwarfs, the absence of an accretion disk can be due to a strong white dwarf magnetic field. When the Alfvén speed, which depends on the local magnetic field strength and the density of the accretion flow is much larger than the Keplerian speed at the circularisation radius, an accretion disk cannot be formed. As an approximation, we may use the criterion:

$$\begin{aligned} \mu_1 \quad &> \quad 1.7 \times 10^{33} \mathrm{G\ cm}^3 \left(\frac{\eta}{0.3}\right) \\ &\times \left(\frac{P_{\rm orb}}{60\ \rm min}\right)^{7/6} \left(\frac{M_1}{M_\odot}\right)^{5/6} \left(\frac{\dot{M}}{10^{18}\ \rm g\ s^{-1}}\right)^{1/2} \end{aligned} \qquad (3)$$

(Wickramasinghe, Wu & Ferrario 1991) to deduce the lower limit to the magnetic moment of the primary star, μ_1, and hence the corresponding limit to the white dwarf polar magnetic field strength. Here, $\dot{M}$ is the accretion rate and η, which approximately equals 0.3, is a parameter which takes into account the angle of the stream as it leaves the inner Lagrangian point (Lubow & Shu 1975).

Using equation 3 we show in Fig. 11 the surface field strength required to equate the Alfvén speed and the Keplerian speed at the circularisation radius, as a function of the accretion rate. We also show the lower limit to the polar magnetic field of the primary white dwarf in binaries for various white dwarf masses M_1 and accretion luminosities L. The orbital period of the binary is fixed at 9.5 min. As shown, if the accreting white dwarf is not massive ($\lesssim 1 M_\odot$ and accretion rate is low ($< 10^{18}$ g s^{-1})), a small polar field ($\lesssim$ 1 MG) is sufficient to prevent the accretion disk formation.

From the *ROSAT* PSPC data, Cropper et al. (1998) deduced that the bolometric accretion luminosity of RX J1914+24 is $\sim 10^{35} - 10^{36}$ erg s^{-1} (for a distance of 100 pc and hydrogen column density $N_{\rm H} \approx 1 \times 10^{22}$ cm^{-2}). If the mass of the primary white dwarf in RX J1914+24 is about 1.0 $M_\odot$, the surface polar field strength of the white dwarf is probably $\gtrsim$ 1MG.

8.2 The synchronising torques

While it is possible that an orbital period longer than the 9.5 min period is hidden in the data, let us assume that RX J1914+24 is indeed synchronised. The geometrical configuration and synchronism of conventional polars have been investigated by many authors (eg Chanmugam & Wagner 1977; Joss, Katz & Rappaport 1979; Lamb et al. 1983;

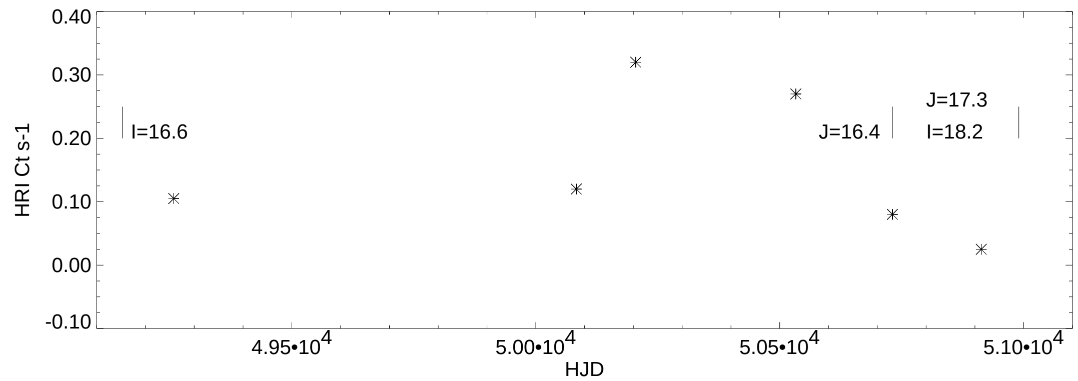

Figure 10. The equivalent *ROSAT* HRI peak count rate as a function of time (HJD-2400000.0).

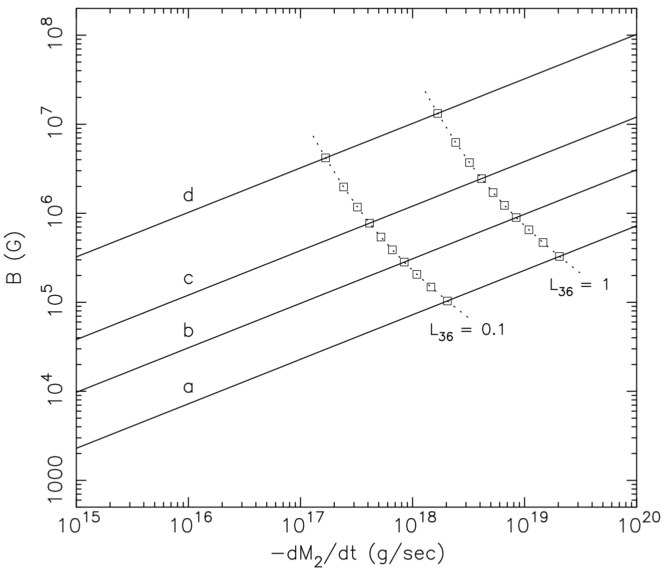

Figure 11. The solid lines a, b, c and d show the relationship between the polar magnetic field strength of the primary white dwarf and the accretion rate such that the Alfvén speed and the Keplerian speed are equal at the circularisation radius for 0.4, 0.7, 1.0 and $1.3M_{\odot}$white dwarfs respectively. These provide a lower limit to the field for diskless accretion. The binary orbital period is fixed at 9.5 min. The open squares show the lower limits to the polar magnetic field strength with masses from 0.4 to $1.3M_{\odot}$(from bottom to top with increments of $0.1M_{\odot}$), for accretion luminosities $L_{36}(=L/10^{36}\mathrm{erg\ s}^{-1})=0.1$ and 1.

Campbell 1983, 1997; Lamb & Melia 1987; King, Frank & Whitehurst 1990; Wu & Wickramasinghe 1993). Some earlier studies (eg Chanmugam & Wagner 1977) implicitly implied that the diskless and synchronisation conditions are equivalent. Although synchronism ensures diskless accretion, diskless accretion may not imply perfect synchronism.

A proper treatment of synchronisation involves magneto-hydrodynamic (MHD) interaction between the stars and the plasma between them (see Campbell 1997) and also the physics of stellar structures of magnetic stars. The issue of synchronisation and formation of ultra-short period double-degenerate binaries is beyond the scope of this paper and deserves a separate study. Here we discuss synchronism in RX J1914+24 briefly only in terms of a crude comparison between the strengths of the accretion torque and the restoring magnetic torques.

The accretion torque which operates about the spin axis of an accreting star is given by

$$\begin{aligned} N_{\mathrm{acc}} &= \frac{2\pi \dot{M} R_{\mathrm{L}}^2}{P_{\mathrm{orb}}} \\ &\approx 2\times 10^{35}\ \mathrm{dyne\ cm} \\ &\quad \times \left(\frac{\dot{M}}{10^{18}\ \mathrm{g/s}}\right)\left(\frac{P_{\mathrm{orb}}}{10\ \mathrm{min}}\right)^{1/3}\left(\frac{M_1}{1.0\ M_{\odot}}\right)^{2/3} \end{aligned} \quad (4)$$

where $P_{\rm orb}$ is the orbital period and $R_{\rm L}$ is the Roche lobe of the star. For a system with an accretion luminosity of about 10^{36} erg s^{-1}, which corresponds to a mass transfer rate of $\sim 10^{18}$ g s^{-1}, the accretion torque is $\sim 10^{35}$ dyne cm. Taking the accretion luminosities deduced in Cropper et al. (1998), we find that the accretion torque on the primary white dwarf in RX J1914+24 is 10 – 100 times that of conventional polars (see Wu & Wickramasinghe 1993). We now investigate whether this exceeds the available synchronising torque.

In conventional polars, the accretion torque is counterbalanced by the magnetic torque and the system maintains synchronism. Two types of magnetic restoring torque have been proposed. The first type is due to the torque arising from magneto-static dipole/multipole interaction between the primary and the secondary star. The second type is due to the torque arising from the MHD interaction between the stars and the plasmas between the stars. In general the second type of torque requires that the secondary star, which is a main-sequence star, has a convective envelope threaded by the magnetic field of the primary degenerate star. Ohmic dissipation occurs at the envelope of the secondary star when the system departs from synchronism.

We can make an estimate of the torque due to magneto-static interaction between the dipole/multipole components of the primary star and the dipole of the secondary star using the equations in Wu & Wickramasinghe (1993). For an orbital period of 9.5 min, the orbital separation is $\sim 10^{10}$ cm. The ratio of orbital separation to the radius of the accreting white dwarf is $\sim$20 for a $1M_{\odot}$white dwarf. For B=10MG and $\mu_1 = 1-10\times 10^{34}$ G cm^3 we find from Wu & Wickramasinghe (1993) that the torque due to magneto-static interaction is of the order of 10^{35} dyne cm or less. (There is some uncertainty since we do not know the magnetic field configuration). This is of the same order or less than the accretion torque (equation 4). Therefore it is not clear if this mechanism alone is able to maintain the synchronism of RX J1914+24.

Degenerate white dwarfs are highly conducting bodies. When synchronism is disturbed, ohmic dissipation occurs much more efficiently in the plasma between the stars than in the stellar envelopes of the white dwarfs. Thus, the large scale MHD instabilities of the field configuration will determine the strength of the restoring magnetic torque (Lamb et al. 1983). According to Lamb & Melia (1988), if both the primary and secondary stars have a non-negligible magnetic moments, the MHD torque acting on the primary star is

$$N_{\rm MHD} \approx 5\times10^{35}\ {\rm dyne\ cm}\left(\frac{\gamma}{0.5}\right)\left(\frac{a}{10^{10}\ {\rm cm}}\right)^{-3} \times\left(\frac{\mu_1}{10^{33}\ {\rm G\ cm}^3}\right)\left(\frac{\mu_2}{10^{33}\ {\rm G\ cm}^3}\right) \qquad (5)$$

where μ_1 and μ_2 are the magnetic moments of the primary and the companion stars respectively, γ is the pitch angle of the dipole magnetic field of the primary star at the companion star, and a is the orbital separation. For the configurations of polars, the value of γ is approximately 1 (Low 1982; Lamb et al. 1983).

For a primary with mass $\sim 1 M_\odot$, Fig. 11 implies that the surface magnetic field of the primary is $\gtrsim$ a few MG if we assume a mass transfer rate similar to that observed by Cropper et al. (1998). This implies a magnetic moment $\mu_1 \sim 10^{34}$ G cm^3. Thus, provided that the secondary star has a similar intrinsic or induced magnetic moment, Equation 5 implies that the MHD synchronising torque is of the order of 5×10^{37} dyne cm. If the mass transfer rate is not much higher than 10^{18} g s^{-1}, the MHD synchronising torque is several order of magnitudes greater than the accreting torque (equation 4) and is able to ensure that the system is in synchronous rotation.

It is worth noting that in deriving equation 4 the magnetic field is ignored and the angular momentum is assumed to be transferred from the accretion flow to the star directly. For a magnetically channeled flow, the interaction between the accretion flow and the star is more complicated. A recent study (Li, Wickramasinghe & Rüdiger 1996) has shown that angular momentum can be transferred from the accretion flow to the star only via the magnetic stress. In non-synchronously rotating systems, the accretion flow interacts with the magnetic field of the accreting star. In polars, as the field lines of the two stars are interconnected, the accretion flow interacts magnetically with both stars. This may allow the angular momentum of the accretion flow to distribute between the two stars and hence to be transferred to the orbit. Thus, equation 4 probably overestimates the strength of these first order considerations of the destabilising torque due to accretion. The synchronism of RX J1914+24 is therefore likely to be more stable than expected from a balance between the MHD torque and the conventional accretion torque.

8.3 Mass transfer rate

The mass transfer in low mass semi-detached binaries is generally driven by the orbital evolution. When the orbital angular momentum of a binary decreases, the orbital separation shrinks, causing matter to overflow the Roche lobe of the secondary star and accrete onto the primary star. For short ($\lesssim$ 3 hr) period systems, gravitational radiation is an efficient process for angular momentum loss, while for long ($\gtrsim$ 3 hr) period systems magnetic braking is the dominant process (eg Verbunt & Zwaan 1981).

Magnetic braking requires the presence of a stellar wind from the secondary star by which the angular momentum is transported. In double-degenerate systems there is no stellar wind. Magnetic braking therefore cannot operate, regardless of the orbital period and whether the system is synchronised or not (see Li, Wu & Wickramasinghe 1994). If RX J1914+24 is indeed a double degenerate system, then the orbital evolution of RX J1914+24 should be solely driven by gravitational radiation.

The mass transfer rate for gravitational-radiation driven orbital evolution is:

$$\dot{M} \approx 1.5\times10^{-6}\ M_\odot/{\rm yr} \times\left[\frac{m_1^2 m_2^2}{(\alpha m_1 - m_2)}\frac{1}{(m_1+m_2)^{1/3}}\right]\left(\frac{P_{\rm orb}}{10\ {\rm min}}\right)^{-8/3} \qquad (6)$$

(cf Faulkner 1971; Wickramasinghe & Wu 1994), where $m_1 = M_1/M_\odot$, $m_2 = M_2/M_\odot$ and $\alpha = 5/6 + n/2$, where n is related by the form $R_2 \propto M_2^n$. For normal stars, $n \sim 1$, giving α=4/3, while for low mass He white dwarfs, $n \sim -1/3$, giving $\alpha \sim 2/3$ (Nauenberg 1972). For $m_1 = 1.0$, $m_2 = 0.08$ (cf §5) and an orbital period of 9.5 mins, the expected mass transfer rate is $\dot{M} \approx 1.8\times10^{-8}\ M_\odot\ {\rm yr}^{-1} \approx 1.1\times10^{18}$ g s^{-1} for a He white dwarf. This is consistent with the value (Cropper et al. 1998) deduced from the ROSAT PSPC data. As mass transfer in RX J1914+24 cannot be driven by magnetic braking or nuclear evolution, the agreement between the observed accretion luminosity and predicted mass transfer rate show evidence of the operation of gravitational radiation in close binaries.

9 CONCLUSIONS

We have found the optical counterpart of RX J1914+24. Our new optical and X-ray data strengthen the suggestion of Cropper et al (1998) that RX J1914+24 is the first known double degenerate polar and has the shortest orbital period of any known binary system. We suggest that the variation in the I band flux is due to the irradiated face of the secondary white dwarf. The long term X-ray light curve shows a variation in flux of an order of magnitude (typical of polars). We estimate that the secondary white dwarf has very low mass ($0.08M_\odot$) and the primary white dwarf has a magnetic field strength greater than a few MG. For double degenerate binaries the dominating synchronising torque is that of MHD interaction between the two stars and the accretion stream while mass transfer is driven solely by gravitational radiation.

10 ACKNOWLEDGMENTS

We would like to thank both the staff of the NOT and the UKIRT for their help at the telescopes. Some of the data presented in this paper have been taken using ALFOSC, which is owned by the Instituto deAstrofisica de Andalucia (IAA) and operated at the Nordic Optical Telescope under agreement between IAA and the NBIfA of the Astronomical Observatory of Copenhagen. UKIRT is operated by the Joint Astronomy Centre on behalf of PPARC. We gratefully acknowledge Darragh O'Donoghue for the use of his period analysis software. KW acknowledges the support from the ARC through an Australian Research Fellowship and PH acknowledges the support from the Academy of Finland.

REFERENCES

Bailey, J., 1981, MNRAS, 197, 31
Barrett, P. E., O'Donoghue, D., Warner, B., 1988, MNRAS, 233, 759
Barstow, M. A., et al, 1993, MNRAS, 254, 16
Barstow, M. A., Dobbie, P. D., Holberg, J. B., Hubeny, I., Lanz, T., 1997, MNRAS, 286, 58
Bessell, M, 1991, PASP, 101, 662
Beuermann, K., Burwitz, V., 1995, In Cape Workshop on magnetic CVs, ASP Con Series, 85, p99, eds Buckley, D. A. H., Warner, B., ASP, San Fransisco
Buckley, D. A. H., Cropper, M. Ramsay, G., Wickramasinghe, D. T., 1998, MNRAS, 299, 83
Campbell, C. G., 1983, MNRAS, 205, 1031
Campbell, C. G., 1997, Magnetohydrodnamics in Binary Stars, Kluwer Academic, Dordrecht
Chanmugam, G., Wagner, R. L., 1977, ApJ, 213, L13
Cropper, M., 1990, Space Sci. Rev., 54, 195
Cropper, M., Harrop-Allin, M. K., Mason, K. O., Mittaz, J. P. D., Potter, S. B., Ramsay, G., 1998, MNRAS, 293, L57
Deeming, T. J., 1975, Astrophys. Space Sci., 36, 137
de Martino, D., Buckley, D. A. H., Mouchet, M., Mukai, K., 1994, A&A, 284, 125
Eggleton, P. P., 1983, ApJ, 268, 368
Faulkner, J., 1971, ApJ, 170, L99
Feigelson, E., Dexter, L., Liller, W., 1978, ApJ, 222, 263
Ferrario, L., Wickramasinghe, D. T., Bailey, J., Tuohy, I. R., Hough, J. H., 1989, ApJ, 337, 832
Fitzpatrick, E. L., 1999, PASP, 111, 63
Frank, J., King, A. R., Raine, D. J., Accretion Power in Astrophysics, CUP, Cambridge
Haswell, C. A., Patterson, J., Thorstensen, J. R., Hellier, C., Skillman, D. R., 1997, ApJ, 476, 847
Iben, I., Tutukov, A., 1991, ApJ, 370, 615
Joss, P. C., Katz, J. I. & Rappaport, S. A., 1979, ApJ, 230, 176
King, A. R., Frank, J., Whitehurst, R., 1990, MNRAS, 244, 731
Kurtz, D. W., 1985, MNRAS, 213, 773
Lamb, D. Q. & Melia, F., 1987, ApJ, 321, L133
Lamb, D. Q. & Melia, F., 1988, in polarized Radiation of Circumstellar Origin, ed Coyne, G. V., Magalhaes, A. M., Moffat, R. E., Schulte-Ladbeck, R. E., Tapia, S., Wickramasinghe, D. T., Vatican Observatory, Vatican City, p45
Lamb, F. K., Aly, J. J., Cook, M. C., Lamb, D. Q., 1983, ApJ, 274, L71
Li, J., Wickramasinghe, D. T., Rüdiger, G., 1996, ApJ, 469, 775
Li, J., Wu, K., Wickramasinghe, D. T., 1994, MNRAS, 268, 61
Livio, M., Pringle, J. E., 1994, ApJ, 427, 956
Low, B. C. 1982, Rev. Geophys. Space Phys., 20, 145
Lubow, S. H., Shu, F. H., 1975, ApJ, 198, 383
Motch, C. et al., 1996, A&A, 307, 459
Nauenberg, M., 1972, ApJ, 175, 417
Patterson, J., 1994, PASP, 106, 209
Ramsay, G., Mason, K. O., Cropper, M., Watson, M. G., Clayton, K., 1994, MNRAS, 270, 692
Ramseyer, T., 1994, ApJ, 425, 243
Southwell, K. A., Still, M. D., Smith, R. C., Martin, J. S., 1995, A&A, 302, 90
Stetson, P., 1992, in Astronomical Data Analysis Software and Systems I, ed Worrall, D. M., Biemesderfer, C., Barnes, J., ASP Conf Series, p297, San Fransisco
Stobie, R. S., Okeke, P. N., Buckley, D. A. H. Buckley, O'Donoghue, D., 1996, MNRAS, 283, L127
Tutukov, A., Yungelson, L., 1996, MNRAS, 280, 1035
Verbunt, F., Zwaan, C., 1981, A&A, 100, L7
Warner, B., 1995, Cataclysmic Variables, CUP
Warwick, R. S., Barber, C. R., Hodgkin, S. T., Pye, J. P., 1993, 262, 289
Wickramasinghe, D. T., Wu, K., Ferrario, L., 1991, MNRAS, 249, 460
Wickramasinghe, D. T., Wu, K., 1994, MNRAS, 266, L1
Wu, K., Wickramasinghe, D. T., 1993, MNRAS, 260, 141
Zombeck, M. V., 1990, Handbook of Astronomy and Astrophysics, 2nd edition, CUP, p100